Desalination and Water Treatment
www.deswater.com
doi: 10.1080/19443994.2014.1003605

57 (2016) 5753–5759
March

Taylor & Francis
Taylor & Francis Group

Adsorption behaviors of ammonium nitrogen by an amphoteric hydrogel

Jia Wei[a], Xuan Liu[b], Shimei Xu[b,*]

[a]*Institute of Commodity Storage and Processing Xinjiang Academy of Agricultural Science, Urumqi, Xinjiang 830091, P.R. China, Tel. +86 991 4536729; email: emma_van001@sina.com*
[b]*Key Laboratory of Oil & Gas Fine Chemicals, Ministry of Education in Xinjiang Uygur Autonomous Region, College of Chemistry and Chemical Engineering, Xinjiang University, Urumqi, Xinjiang 830046, P.R. China, Tel. +86 991 8581870; emails: xushmei@gmail.com (X. Liu), xushmei@hotmail.com (S. Xu)*

Received 26 February 2014; Accepted 28 December 2014

ABSTRACT

An amphoteric hydrogel was prepared by cross-linking graft copolymerization of dimethyldiallylammonium chloride and acrylic acid onto soluble starch. The adsorption behaviors of ammonium nitrogen (NH_4^+-N) by the amphoteric hydrogel were discussed in this study. The effects of various experimental parameters on NH_4^+-N removal, including pH, the dose of absorbent, the temperature, the adsorption time, and the initial concentration of NH_4^+-N, were investigated. The result indicated that the amphoteric hydrogel showed a fast adsorption rate and high adsorption capacity for NH_4^+-N in a pH range from 4 to 8. The adsorption process was exothermic according to the value of thermodynamic parameters. The adsorption process fits the pseudo-second-order kinetic model best. To this hydrogel, it was seen that the Freundlich adsorption isotherm model fits the adsorption data better. The adsorption capacity could reach to 33.98 mg/g. The hydrogel showed the potential use for removal of NH_4^+-N in water treatment and fishing industry.

Keywords: Adsorption; Hydrogel; Ammonium nitrogen; Amphoteric; Starch; Removal

1. Introduction

Hydrogels are three-dimensional cross-linked polymers and widely used in many fields, such as absorbents, sensors, drug delivery materials, etc. due to its prominent water-absorbing and water-retaining performance. The uses of absorbent hydrogels as adsorbents for the removal of dyes [1,2], heavy metal ions [3,4], and toxic components [5,6] have been paid much more attention in recent years.

Ammonium nitrogen (NH_4^+-N) is a common ion existing in domestic sewage, chemical engineering, petrochemical industry, fertilizer industry, and metallurgy industrial sewage. As one of the nutrient ions in the water, a high concentration of NH_4^+ ion would be fatal to aquatic animals due to the formation of NH_3 by hydrolysis.

$$NH_4^+ + OH^- \leftrightarrow NH_3 + H_2O$$

Some methods had been developed for removal of NH_4^+, such as ion exchange [7], biological treatment [8], membrane processes [9], air-stripping [10], and adsorption [11,12]. Among which, the adsorption technology has been extensively studied and considered to be effective and efficient. Zeolite or molecular sieve, however, was not satisfying as a naturally available

---

*Corresponding author.

adsorbent. Instead, hydrogels were developed to show an effective adsorption on ammonium nitrogen. Yuan and Kusuda [13] prepared a hydrogel poly(N-isopropylacrylamide-co-chlorophyllin) with an adsorption capacity of 0.18 mg/g for NH_4^+-N. Zheng et al. [14] group developed a series of chitosan-grafted poly (acrylic acid)/unexpanded vermiculite (CTS-g-PAA/UVMT) hydrogel with a maximum adsorption capacity of 21.7 mg/g for NH_4^+-N.

In the adsorption process, for the hydrogels, the functional groups such as amino or carboxyl groups in the adsorbents played an important role in determining the effectiveness, selectivity, and reusability of the adsorbent materials [15–17]. Furthermore, adsorbents with amino groups showed bifunctional properties [18,19] which enabled them to adsorb cationic and anionic target compounds at different pH values in aqueous solutions. However, most of hydrogels were anionic for the removal of NH_4^+-N and thus were only effective on the removal of specific cations. Besides, the removal efficiency usually decreased due to salt sensitivity of the anionic hydrogels.

In previous research, the amphoteric absorbents were used for the removal of both anionic and cationic metal ions [20,21] and dyes [22,23]. The amphoteric absorbents were proven to be effective on adsorption of both cations and anions in water [24]. So in the present work, amphoteric hydrogels were chosen to be studied in this article due to their good salt tolerance [25].

Soluble starch was chosen owing to its biodegradable, low-cost, and biocompatible characteristic. Dimethyldiallylammonium chloride (DMDAAC) and acrylic acid (AA) carried out a cross-linking graft copolymerization into a soluble starch matrix. The obtained hydrogel was used to remove NH_4^+ ions from aqueous solution, and various factors such as pH, absorbent dose, adsorption time, temperature, the initial concentration of the hydrogel were investigated in this study.

2. Materials

The following were used in this study: Soluble starch (Hutubi, Xinjiang), sodium hydroxide, (AA, Tianjin Guangfu Chemical Reagent Factory, Tianjin, China), (DMDAAC, 60 wt.% aqueous solution, Shandong Luyue Chemical Co., Shandong, China), *N*, *N*′-methylene bisacrylamide (MBAM, Shanghai Chemical Co., Shanghai, China), ammonium persulfate (ASP, Xi'an Chemical Co., Xi'an, China), ammonium chloride (guarantee reagent, Sinopharm Chemical Reagent Co., Ltd, China), hydrochloric acid (Sichuan Xilong Chemical Reagent Factory, Sichuang, China), ethanol alcohol (Tianjin Zhiyuan Reagent Co., Ltd, Tianjin, China). All the reagents used in this study were analytical reagent, and all solutions were prepared with deionized water.

3. Preparation of amphoteric hydrogel

The AA was neutralized by 30 wt.% of NaOH solution to a neutralization degree of 75 mol% in an ice bath. 1 g of soluble starch was dissolved in 15 mL of distilled water, and then, 15 mL of neutralized AA and 2 g of DMDAAC were added. Afterward, 0.09% of MBAM (based on the weight of AA) and 2.5% of ASP (based on the weight of AA) were added to the solution above before the temperature rose to 50℃. The gel point appeared after 30 min, and then, the system temperature rose to 100℃ for another 2 h. The resulting product was immersed in excess deionized water to remove the unreacted monomers in the gel and then dehydrated with absolute ethanol and dried at 100℃ to a constant weight. The hydrogel was milled through 80- to 100-mesh screen before use.

4. Adsorption procedure

The absorption experiment was carried out in a series of Erlenmeyer flask filled with absorbents in a dose range of 20–60 mg and 50.00 mL of 50 mg/L NH_4Cl aqueous solution. The pH of the initial solution (pH 7) was adjusted by 0.1 mol/L HCl or NaOH. After vibrating about 2 h, the hydrogel was taken out and the amount of residual NH_4^+ ions was determined by ultraviolet spectrophotometer (Puxitongyong TU-1810) according to Nessler's reagent colorimetric method. The adsorption capacity of hydrogel absorbent was calculated by the following expression:

$$Q\ (\mathrm{mg/g}) = \frac{(c_0 \times V_0 - c_e \times V_e)}{m} \tag{1}$$

where the Q is the equilibrium adsorption capacity of absorbent, the C_0 (mg/L) and C_e (mg/L) are the initial and equilibrium concentration of NH_4^+, respectively, the V_0 (mL) and V_e (mL) are the volumes of NH_4^+ before and after the absorption, respectively, m (g) is the amount of dried hydrogel absorbent.

5. Result and discussion

The synthesis procedure of hydrogel was illustrated in Fig. 1. The resultant amphoteric hydrogels contained both carboxyl groups and ammonium groups. So it was expected that the amphoteric

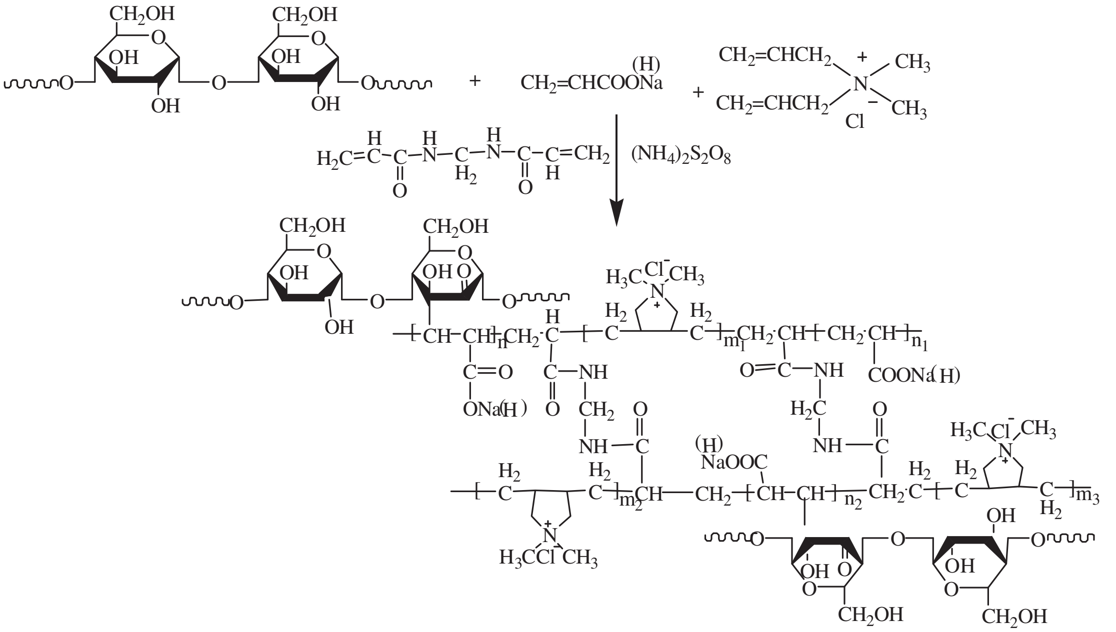

Fig. 1. The preparation of amphoteric hydrogel.

hydrogel would be effective for the removal of both cationic and anionic ions since the adsorption process was driven by electrostatic interaction.

FT-IR spectra of the amphoteric hydrogel (Fig. 2(a)) and soluble starch (Fig. 2(b)) were shown in Fig. 2. The strong peaks occurred at 3,436, 2,943, and 1,676 cm^{-1} due to the stretching vibration of –H, C–H, and –COOH groups in amphoteric hydrogel, respectively. The peak at 852 cm^{-1} resulted from the typical peak of starch. Cationic groups were not found in the spectrum due to lack of obvious characteristic peak. The subsequent experiments to azophloxine dye had proved the existence of cationic ions in the amphoteric hydrogel.

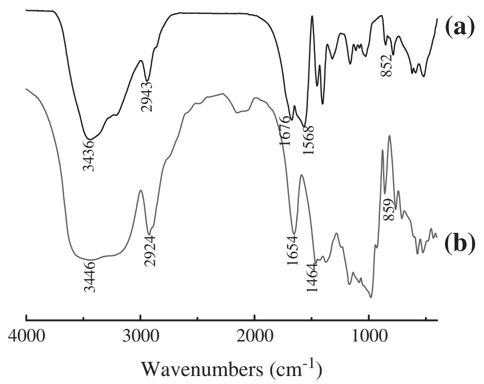

Fig. 2. FT-IR spectra of amphoteric hydrogel (a) and soluble starch (b).

The SEM was used to describe the inner appearance of the amphoteric hydrogel. Generally speaking because the evaporation during the drying process makes the pores in the hydrogel collapse, it is difficult to judge the appearance of swollen hydrogel. But the swelling hydrogel can maintain its original shape after freeze-drying, the actually inner appearance of hydrogel could be observed. The hydrogel evidently shows the space network structure in the Fig. 3. The pores are well distributed, the size is about 20 μm, and this rough structure can facilitate the adsorption.

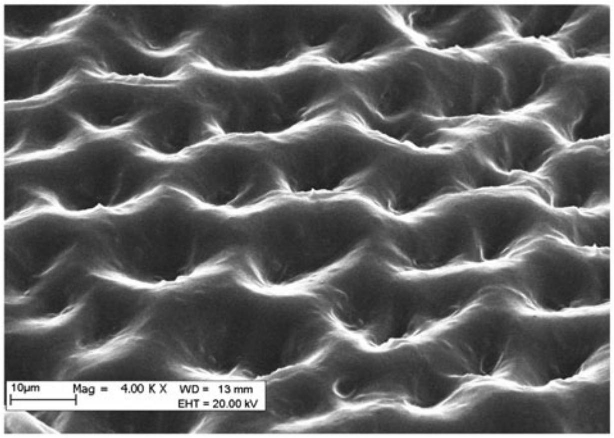

Fig. 3. SEM of hydrogel.

5.1. The effect of pH

pH value was one of the most critical factors on influencing the adsorption capacity of hydrogels. Fig. 4 showed the effect of pH value on adsorption capacity of NH_4^+. It can be seen clearly that the adsorption capacity slowly increased at a wide pH range of 4.0–8.0 and reached the maximum at pH of 8.0. When the pH value increased to 10, a sharp drop in adsorption capacity was observed. In this study, the absorption process was driven by electrostatic attraction between negatively charged carboxymethyl groups in the hydrogel and positively charged NH_4^+ groups in the ammonium chloride solution. The process, however, was also influenced by the swelling behaviors of the hydrogel. At the low pH value, carboxymethyl groups were protonated and appeared as $–CH_2COOH$, reducing the chance of the NH_4^+ absorbing into the hydrogel. Besides, the hydrogel shrank due to reduced electrostatic repulsive force between carboxymethyl groups. This made it hard for NH_4^+ to diffuse into the hydrogel, so led to a low adsorption. With the increasing of pH, –COOH was deprotonated into $–COO^-$, so the active sites of adsorption increased and the hydrogel swell. As a result, a high adsorption was observed. However, at the higher pH values, the hydrolyzation of NH_4^+ would take place and NH_3 was the main form in the aqueous solution, resulting in a decreasing equilibrium adsorption capacity for NH_4^+ instead.

5.2. The effect of dose of hydrogel

The equilibrium adsorption capacity of NH_4^+ under different absorbent doses in a range of 20–60 mg was shown in Fig. 5. The equilibrium adsorption capacity decreased when the dose of absorbent increased, while the equilibrium concentration C_e decreased from 35.76 to 22.22 mg/L. The equilibrium adsorption capacity of NH_4^+-N heavily depended on the number of $–COO^-$ groups. Usually, the larger the number of $–COO^-$ groups was, the bigger the adsorption capacity of NH_4^+ in theory. However, the $–COO^-$ groups of the hydrogel may not be fully occupied by NH_4^+ since the polymer chains in the hydrogel were not fully expanded. Another reason was the repulsion of ammonium groups inside the hydrogel, which blocked the approach of NH_4^+ to the $–COO^-$ groups.

5.3. Adsorption isotherm

The adsorption capacity of NH_4^+ with varying temperature from 20 to 50℃ was shown in Fig. 6. As the temperature rose, the adsorption capacity basically indicated no obvious changes.

To investigate the adsorption isotherm, the free energy (ΔG^θ), enthalpy (ΔH^θ), and entropy (ΔS^θ) were calculated, respectively, according to the Van's Hoff and thermodynamic equation. The values of ΔG^θ, ΔH^θ, and ΔS^θ were listed in Table 1. The result showed that the adsorption process was exothermic because of the negative value of ΔH^θ. Furthermore, a negative value of ΔG^θ indicated the NH_4^+ adsorption process was easy to occur.

$$\log\left(\frac{Q}{Ce}\right) = -\frac{\Delta H^\theta}{2.303RT} + \frac{\Delta S^\theta}{2.303R} \tag{2}$$

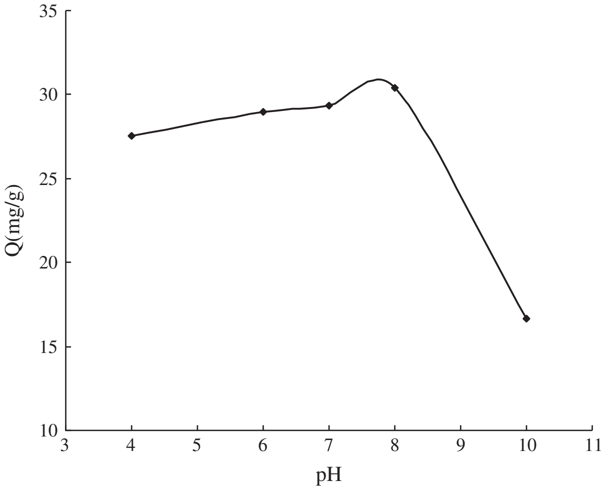

Fig. 4. The effect of pH on the adsorption capacity of amphoteric hydrogels: $C_0 = 50$ mg/L; $t = 2$ h; $T = 25$℃; absorbent dose = 30 mg; 140 rpm.

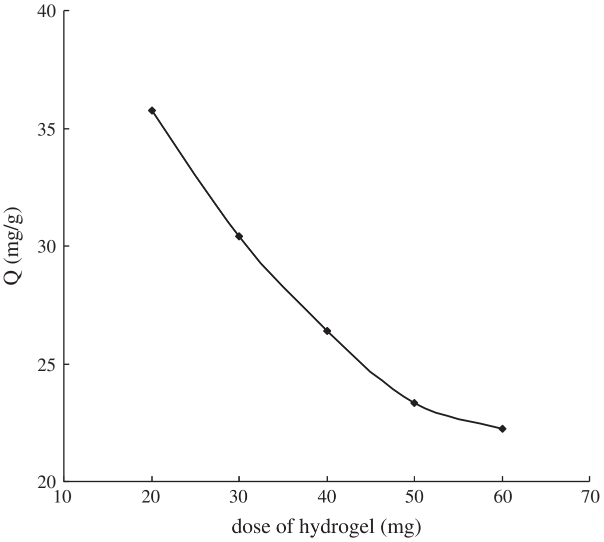

Fig. 5. The effect of dose on the adsorption capacity of amphoteric hydrogels: $C_0 = 50$ mg/L; pH 8.03; $t = 2$ h; $T = 25$℃; 140 rpm.

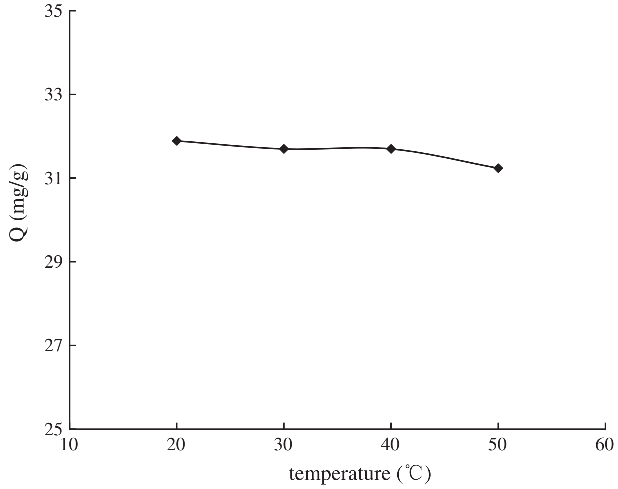

Fig. 6. The effect of temperature on the adsorption capacity of amphoteric hydrogels: $C_0 = 50$ mg/L; pH 8.03; absorbent dose = 30 mg; $t = 2$ h; 140 rpm.

$$\Delta G^\theta = \Delta H^\theta - \mathrm{T}\Delta S^\theta \tag{3}$$

where R is a constant (8.314 J/k mol)) and T is absolute temperature.

The Fig. 7 showed the effect of the initial concentration of NH_4^+ at 25℃. As the initial concentration increased from 20 to 70 mg/L, the equilibrium adsorption capacity increased from 16.69 to 42.82 mg/g, respectively. A high initial concentration of NH_4Cl provided more probability of contacts between ions in the solution and active sites on hydrogel surface [26]. It facilitated the diffusion of NH_4^+ into hydrogel and bound to –COO$^-$ groups.

It is necessary to study the equilibrium adsorption isotherm because it shows the adsorption ability of an absorbent. According to isotherm model, the different adsorption parameters can be calculated which indicated the surface properties and the appeal of an adsorption for adsorbent. In this adsorption process, Freundlich adsorption isotherm model was best to describe the absorption model of NH_4^+.

Table 1
Thermodynamic value at various temperatures

Temperature (℃)	Q (mg/g)	ΔG^θ (kJ/mol)	ΔH^θ (kJ/mol)	ΔS^θ (J/mol K)
20	31.890	−5.345	−1.676	12.516
30	31.698	−5.470		
40	31.698	−5.596		
50	31.238	−5.721		

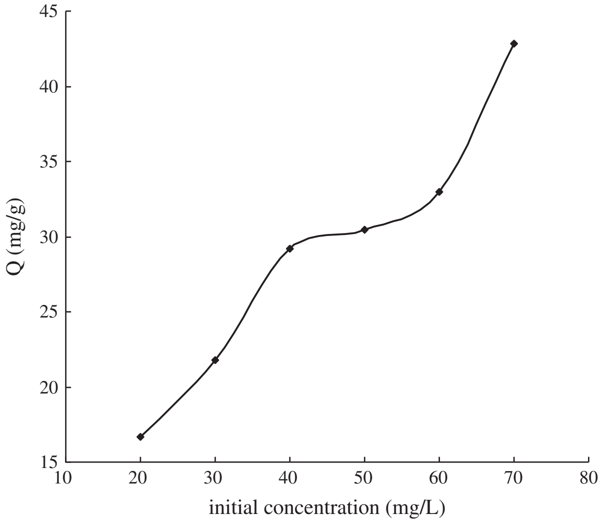

Fig. 7. The effect of initial concentration on the adsorption capacity of amphoteric hydrogels: pH 8.04; $T = 25$℃; absorbent dose = 30 mg; $t = 2$ h; 140 rpm.

$$\text{Freundlich equation: } \ln Q = \ln K + \frac{1}{n} \ln C_\mathrm{e} \tag{4}$$

where Q (mg/g) is the monolayer adsorption capacity of the adsorbent, K (L/g) is a constant related to the adsorption capacity, and n is an empirical parameter related to the adsorption intensity. The values of K, n, and correlation coefficient R^2 are 3.841 (L/g), 1.689, and 0.9375, respectively.

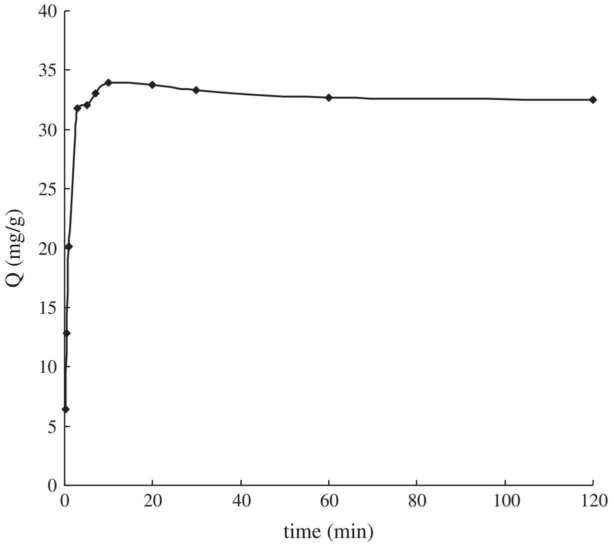

Fig. 8. The effect of time on the adsorption capacity of amphoteric hydrogels: $C_0 = 50$ mg/L; pH 8.12; $T = 25$℃; absorbent dose = 30 mg; 140 rpm.

Table 2
The adsorption model and capacity for NH_4^+-N onto different adsorbents

Absorbent	Isotherm Model	Pseudo-second-order model		References
		k (g/mg min)	Q_m (mg/g)	
Natural zeolite	Freundlich	0.185	3.328	[28]
Zeolite (low-calcium)	Langmuir	3.63×10^{-2}	23.8	[29]
Natural Turkish clinoptilolite	Langmuir	3×10^{-2}	5.95	[13]
Microwave-treated zeolite	Langmuir–Freundlich	0.162	11.59	[30]
PVA/PAA/Tm	Langmuir model	2.87×10^{-2}	32.36	[12]
CTS/PAA/APT	Dubinin–Radushkevich model	7.70×10^{-2}	20.46	[31]
Zeolite 13X	Freundlich and Dubinin–Radushkevich	0.681	4.81	[32]
DMDAAC/AA/starch	Freundlich	1.38×10^{-2}	47.17	This study

When contacting the solution, the three-dimensional network of the hydrogel began to expand due to the electrostatic repulsion and hydrophility of carboxyl or ammonium groups in the hydrogel, which made more solvent molecular diffusing into the inner part of the adsorbent. The electrostatic repulsion between NH_4^+-N and ammonium groups in the hydrogel became larger accompanying with more NH_4^+-N attracted by carboxyl groups in the hydrogel. When the electrostatic repulsion and attraction came to a balance, the adsorption process reached equilibrium too. So the adsorption of NH_4^+ onto the hydrogel was mainly driven by the electrostatic force.

5.4. The effect of time

Generally, the adsorption of ions in aqueous solution consists of three steps: (1) the ions from the bulk solution diffuse through the liquid to the surface of hydrogel; (2) the ions diffuse into the active sites of hydrogel; and (3) the ions are absorbed on the active site due to the electrostatic attraction [27]. In the experiment, the absorption process rapidly reached equilibrium in the initial 10 min (Fig. 8). The pseudo-second-order kinetic model was used to obtain the mechanism parameters for NH_4^+.

$$\frac{1}{Q_t} = \frac{1}{kQ_m^2 t} + \frac{1}{Q_m} \quad (5)$$

here Q_t is the adsorption capacity at time t (min), Q_m is the adsorption capacity, and k is the rate constant of the pseudo-second-order. The value of Q_m and k was shown in Table 2.

In addition, the equilibrium adsorption capacity was compared with other adsorbents reported. The data were listed in Table 2. Obviously, this hydrogel possessed much higher adsorption capacity for NH_4^+-N, making it to be a potential and reliable adsorbent for NH_4^+-N removal from aqueous solution.

6. Conclusion

The adsorption process of NH_4-N by an amphoteric hydrogel was investigated in this study. The hydrogel showed appreciable adsorption ability for NH_4^+-N at the pH range of 4–8. The equilibrium adsorption capacity decreased as the dose of hydrogel increased, but the change of temperature did not seem to affect the adsorption capacity very well in a range of 20–50°C. The adsorption reached equilibrium within 10 min and fits the pseudo-second-order kinetic model. The adsorption process was exothermic, and the adsorption isotherm was well described by Freundlich isotherm model. The amphoteric hydrogel showed a maximum capacity of 33.98 mg/g for the adsorption of NH_4^+-N. Due to its effectiveness and efficiency, the hydrogel showed a potential application in the field of water treatment and fishing industry.

Acknowledgments

This work was supported by the Startup Foundation for Doctors of Xinjiang University, China [BS100116].

References

[1] N.B. Shukla, S. Rattan, G. Madras, Swelling and dye-adsorption characteristics of an amphoteric superabsorbent polymer, Ind. Eng. Chem. Res. 51 (2012) 14941–14948.

[2] R. Bhattacharyya, S.K. Ray, B. Mandal, A systematic method of synthesizing composite superabsorbent hydrogels from crosslink copolymer for removal of textile dyes from water, J. Ind. Eng. Chem. 19 (2013) 1191–1203.

[3] C. Demirbilek, C.Ö. Dinç, Synthesis of diethylaminoethyl dextran hydrogel and its heavy metal ion adsorption characteristics, Carbohydr. Polym. 90 (2012) 1159–1167.

[4] W.B. Wang, Y.R. Kang, A.Q. Wang, One-step fabrication in aqueous solution of a granular alginate-based hydrogel for fast and efficient removal of heavy metal ions, J. Polym. Res. 20 (2013) 1–10.

[5] N. Sahiner, O. Ozay, N. Aktas, Aromatic organic contaminant removal from an aqueous environment by p(4-VP)-based materials, Chemosphere 85 (2011) 832–838.

[6] H.H. Sokker, N.M. El-Sawy, M.A. Hassan, B.E. El-Anadouli, Adsorption of crude oil from aqueous solution by hydrogel of chitosan based polyacrylamide prepared by radiation induced graft polymerization, J. Hazard. Mater. 190 (2011) 359–365.

[7] R. Leyva-Ramos, J.E. Monsivais-Rocha, A. Aragon-Piña, M.S. Berber-Mendoza, R.M. Guerrero-Coronado, P. Alonso-Davila, J. Mendoza-Barron, Removal of ammonium from aqueous solution by ion exchange on natural and modified chabazite, J. Environ. Manage. 91 (2010) 2662–2668.

[8] S.F. Zhang, Y.Y. Wang, W.T. He, M. Wu, M.Y. Xing, J. Yang, N.Y. Gao, D.Q. Yin, Responses of biofilm characteristics to variations in temperature and NH_4^+-N loading in a moving-bed biofilm reactor treating micro-polluted raw water, Bioresour. Technol. 131 (2013) 365–373.

[9] A. Hasanoğlu, J. Romero, B. Pérez, A. Plaza, Ammonia removal from wastewater streams through membrane contactors: Experimental and theoretical analysis of operation parameters and configuration, Chem. Eng. J. 160 (2010) 530–537.

[10] S. Guštin, R. Marinšek-Logar, Effect of pH, temperature and air flow rate on the continuous ammonia stripping of the anaerobic digestion effluent, Process Saf. Environ. Prot. 89 (2011) 61–66.

[11] D. Karadag, Y. Koc, M. Turan, B. Armagan, Removal of ammonium ion from aqueous solution using natural Turkish clinoptilolite, J. Hazard. Mater. 136 (2006) 604–609.

[12] Y.A. Zheng, Y. Liu, A.Q. Wang, Fast removal of ammonium ion using a hydrogel optimized with response surface methodology, Chem. Eng. J. 171 (2011) 1201–1208.

[13] L.J. Yuan, T. Kusuda, Adsorption of ammonium and nitrate ions by poly(N-isopropylacrylamide) gel and poly(N-isopropylacrylamide-co-chlorophyllin) gel in different states, J. Appl. Polym. Sci. 96 (2005) 2367–2372.

[14] Y.A. Zheng, Y.T. Xie, A.Q. Wang, Rapid and wide pH-independent ammonium-nitrogen removal using a composite hydrogel with three-dimensional networks, Chem. Eng. J. 179 (2012) 90–98.

[15] H.Y. Ao, M.L. Huang, J.H. Wu, J.M. Lin, Q.W. Tang, H. Sun, Synthesis and properties of poly(acrylamide-co-acrylic acid)/polyacrylamide superporous IPN hydrogels, Polym. Adv. Technol. 20 (2009) 1044–1049.

[16] Z.B. Chen, F. Dong, M.Z. Liu, X.H. Qi, Preparation and properties of porous poly(sodium acrylate-co-acrylamide) salt-resistant superabsorbent composite, Polym. Eng. Sci. 51 (2011) 2453–2464.

[17] F. Li, C.L. Bao, J.H. Zhang, Q. Sun, W.W. Kong, X.Y. Han, Y. Wang, Synthesis of chemically modified chitosan with 2,5-dimercapto-1,3,4-thiodiazole and its adsorption abilities for Au(III), Pd(II), and Pt(IV), J. Appl. Polym. Sci. 113 (2009) 1604–1610.

[18] Y.F. Lin, H.W. Chen, P.S. Chien, C.S. Chiou, C.C. Liu, Application of bifunctional magnetic adsorbent to adsorb metal cations and anionic dyes in aqueous solution, J. Hazard. Mater. 185 (2011) 1124–1130.

[19] S.H. Huang, D.H. Chen, Rapid removal of heavy metal cations and anions from aqueous solutions by an amino-functionalized magnetic nano-adsorbent, J. Hazard. Mater. 163 (2009) 174–179.

[20] S.M. Xu, S.F. Zhang, R.W. Lu, J.Z. Yang, C.X. Cui, Study on adsorption behavior between Cr(VI) and crosslinked amphoteric starch, J. Appl. Polym. Sci. 89 (2003) 263–267.

[21] S.M. Xu, S. Feng, F. Yue, J.D. Wang, Adsorption of Cu (II) ions from an aqueous solution by crosslinked amphoteric starch, J. Appl. Polym. Sci. 92 (2004) 728–732.

[22] S.M. Xu, J.L. Wang, R.L. Wu, J.D. Wang, H. Li, Adsorption behaviors of acid and basic dyes on crosslinked amphoteric starch, Chem. Eng. J. 117 (2006) 161–167.

[23] S.M. Xu, J.L. Wang, R.L. Wu, J.D. Wang, Effect of degree of substitution on adsorption behavior of Basic Green 4 by highly crosslinked amphoteric starch with quaternary ammonium and carboxyl groups, Carbohydr. Polym. 66 (2006) 55–59.

[24] S.M. Xu, R.L. Wu, X.J. Huang, L.Q. Cao, J.D. Wang, Effect of the anionic-group/cationic-group ratio on the swelling behavior and controlled release of agrochemicals of the amphoteric, superabsorbent polymer poly (acrylic acid-co-diallyldimethylammonium chloride), J. Appl. Polym. Sci. 102 (2006) 986–991.

[25] C.L. Fei, D.Q. Huang, S. Feng, Adsorption behavior of amphoteric double-network hydrogel based on poly (acrylic acid) and silica gel, J. Polym. Res. 19 (2012) 9929.

[26] Z.H. Ai, Y. Cheng, L.Z. Zhang, J.R. Qiu, Efficient removal of Cr(VI) from aqueous solution with Fe@Fe_2O_3 core−shell nanowires, Environ. Sci. Technol. 42 (2008) 6955–6960.

[27] S.M. Xu, J. Wei, S. Feng, J.D. Wang, X.S. Li, A study in the adsorption behaviors of Cr(VI) on crosslinked cationic starches, J. Polym. Res. 11 (2004) 211–215.

[28] N. Widiastuti, H.W. Wu, H.M. Ang, D.K. Zhang, Removal of ammonium from greywater using natural zeolite, Desalination 277 (2011) 15–23.

[29] M.L. Zhang, H.Y. Zhang, D. Xu, L. Han, D.X. Niu, L.Y. Zhang, W.S. Wu, B.H. Tian, Ammonium removal from aqueous solution by zeolites synthesized from low-calcium and high-calcium fly ashes, Desalination 277 (2011) 46–53.

[30] L.C. Lei, X.J. Li, X.W. Zhang, Ammonium removal from aqueous solutions using microwave-treated natural Chinese zeolite, Sep. Purif. Technol. 58 (2008) 359–366.

[31] Y.A. Zheng, J.P. Zhang, A.Q. Wang, Fast removal of ammonium nitrogen from aqueous solution using chitosan-g-poly(acrylic acid)/attapulgite composite, Chem. Eng. J. 155 (2009) 215–222.

[32] A. Arslan, S. Veli, Zeolite 13X for adsorption of ammonium ions from aqueous solutions and hen slaughterhouse wastewaters, J. Taiwan Inst. Chem. Eng. 43 (2012) 393–398.